New Journal of Physics
An Institute of Physics and Deutsche Physikalische Gesellschaft Journal

Microwave spectroscopy on a double quantum dot with an on-chip Josephson oscillator

A W Holleitner†, H Qin†, F Simmel†, B Irmer†, R H Blick†, J P Kotthaus†, A V Ustinov‡ and K Eberl§

† Center for NanoScience and Sektion Physik,
Ludwig-Maximilians-Universität, Geschwister-Scholl-Platz 1, 80539 München, Germany
‡ Physikalisches Institut III, Universität Erlangen–Nürnberg,
Erwin-Rommel-Strasse 1, 91058 Erlangen, Germany
§ Max-Planck-Institut für Festkörperforschung, Heisenbergstrasse 1,
70569 Stuttgart, Germany
E-mail: robert.blick@physik.uni-muenchen.de

New Journal of Physics **2** (2000) 2.1–2.7 (http://www.njp.org/)
Received 19 November 1999; online 18 February 2000

Abstract. We present measurements on microwave spectroscopy on a double quantum dot with an on-chip microwave source. The quantum dots are realized in the two-dimensional electron gas of an AlGaAs/GaAs heterostructure and are weakly coupled in series by a tunnelling barrier forming an 'ionic' molecular state. We employ a Josephson oscillator formed by a long Nb/Al–AlO_x/Nb junction as a microwave source. We find photon-assisted tunnelling sidebands induced by the Josephson oscillator, and compare the results with those obtained using an externally operated microwave source.

Microwave spectroscopy on quantum dots allows us to probe the dynamics of these few-electron systems. Most of the experimental work conducted to date has been focussed on rather simple spectroscopic tools: a microwave signal is coupled via an antenna or a stripline to the mesoscopic system under test. The photon-induced current through the dots is measured and allows the discrete states of the quantum system to be probed directly [1, 2, 3]. These results can be described by the Tien–Gordon theory [4], originally developed for a superconductor tunnel junction, and more recent theoretical models [5, 6, 7, 8]. However, in order to reveal the dynamics of electrons confined in tunnel-coupled dot systems, more intricate spectroscopic tools are required. Nakamura *et al* [9] showed how to monitor a single tunnelling Cooper pair in a superconducting tunnel junction transistor in the time domain. This has spurred interest in tracing electrons in coupled quantum dots, since in this case a similar tunnel splitting of the discrete states was found [10, 11].

PII: S1367-2630(00)09731-7
1367-2630/00/000002+7$30.00

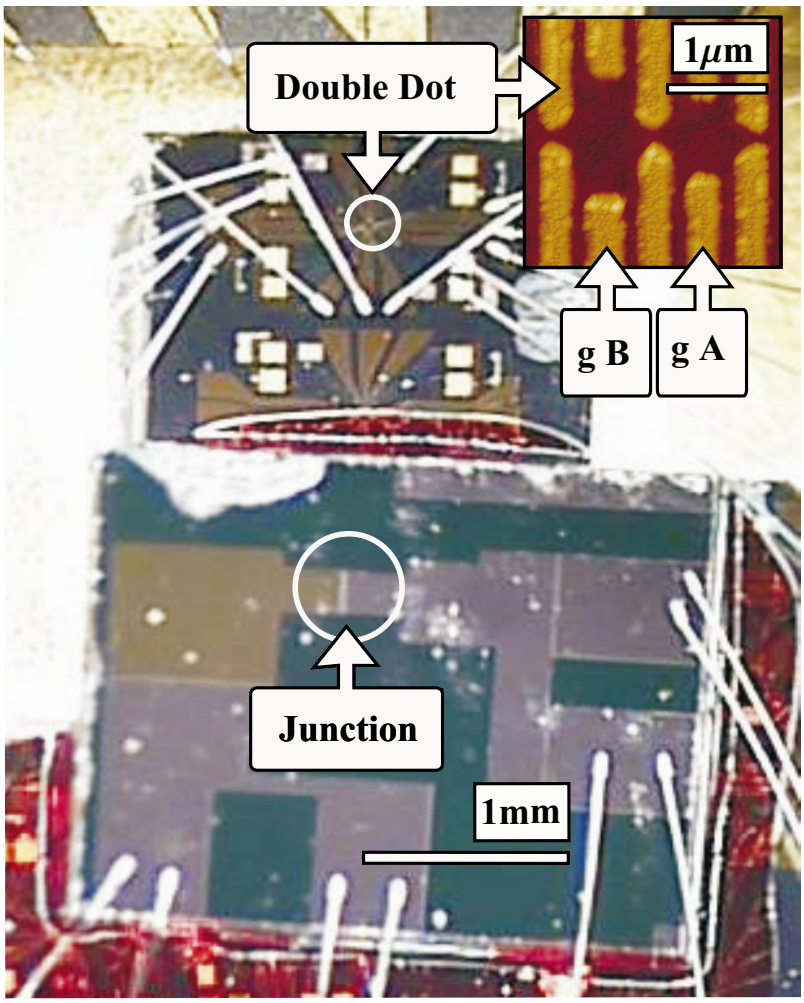

Figure 1. Top view of the circuit: the quantum dots are located in the centre of the Hall bar (marked by the upper white circle). The inset (top right) shows an AFM micrograph of the gates used to form the double dots (gB and gA are the plunger gates operated during the measurements). The Josephson oscillator is placed on top of the quantum dot chip and glued to it with photoresist. The lower white circle indicates the position of the junction itself. Radiation is coupled through the GaAs substrate to the quantum dots (see text for details).

Here we present an on-chip microwave oscillator integrated in a single low-temperature set-up with a coupled quantum dot structure. Integrating on-chip microwave sources has the advantage of easily combining advanced spectrometers with mesoscopic devices. Furthermore, the influence of black-body radiation is minimized, since all the electrical connections to the outside world are essentially dc lines and so can be heavily filtered [12, 13]. As a microwave source we employ a long Josephson tunnel junction (JTJ) with well-defined emission characteristics. These junctions commonly radiate in the range from a few GHz up to 600 GHz [14]. Their typical radiation linewidth can be as small as 10^{-6} relative to the emission frequency [15]. Recently, this has triggered rapid progress in the use of these devices in integrated submillimetre wave superconducting receivers [16]. The quantum dots are defined in

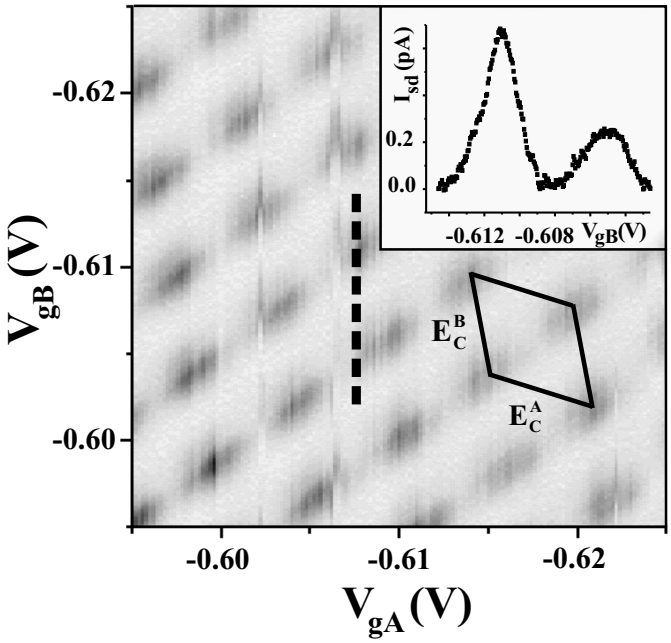

Figure 2. Charging diagram of the double quantum dot as a greyscale plot without microwave radiation (white: I = 0 pA, black: $I > 0.5$ pA). A small forward bias of V_{ds} = 19 μV is applied to monitor the current. The two dots are weakly coupled by the tunnel barrier and produce a periodic lattice. E_C^A and E_C^B denote the charging energies, illustrated by the diamond. The two gate voltages V_{gA} and V_{gB} span the charging diagram. The inset shows a line plot of the dc current through the double dot. The range of voltage V_{gB} in this graph coincides with the broken line in the greyscale plot.

a two-dimensional electron gas (2DEG) by electron-beam-written lateral Schottky gates. The versatility of these devices lies in their ability to tune the tunnel contacts over a wide range. This permits the straightforward fabrication of tunnel-coupled quantum dots ('covalent artificial molecules') or decoupled dots ('ionic artificial molecules') [11].

In contrast to the excitation spectra of real atoms or molecules, the spectra of single or even coupled quantum dots reveal a striking difference in their discrete level structures. It has been shown in a whole variety of experiments that Kohn's theorem [17] prevails for quantum dots [18, 19]. The theorem states that only the centre-of-mass (CM) degree of freedom couples to a spatially homogeneous electromagnetic field. In previous studies of excitations in quantum dots by coupling radiation via antennas, only CM excitations were found [11, 19, 20]. Here we 'move' the radiation source close to the quantum dots in an attempt to verify whether the inhomogeneity of the near-field radiation affects the electronic excitations. This is in close analogy to the probing of single molecules by scanning near-field microscopy [21].

Our set-up is shown in figure 1: the Si chip with the Nb/Al–AlO_x/Nb Josephson junction is glued on top of the quantum dot AlGaAs/GaAs chip with photoresist. The inset of figure 1 shows the quantum dot gate structure used in this work: the application of an appropriate negative gate voltage defines two quantum dots in the 2DEG of the AlGaAs/GaAs heterostructure with an electron density of 1.7 $\times 10^{15}$ m^{-2} at 35 mK (marked by the upper white circle in figure 1). By

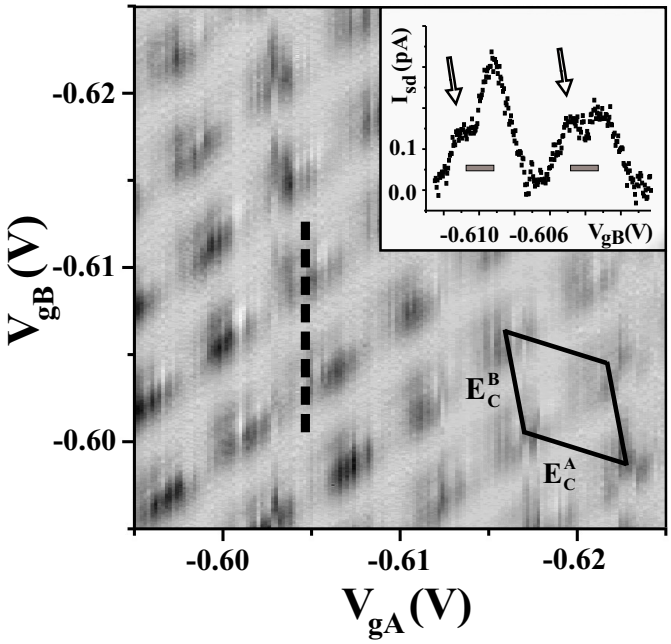

Figure 3. Charging diagram with an identical scan range to figure 2, but under microwave radiation from a far-field source at 10 GHz. The sidebands appear on only one side, depending on the tuning of the tunnel barriers. Inset: photocurrent with the sidebands induced by the frequency-dependent absorption. Pumping of the electrons leads to a reduction of the absolute current value. The grey bars denote the range of voltage V_{gB} which corresponds to the frequency of f = 10 GHz on this axis.

varying the voltages V_{gA} and V_{gB} applied to the plunger gates shown in the inset of figure 1, the electron configuration of the double dot can be changed. Plotting the current through the system as a function of V_{gA} and V_{gB} produces the charging diagram in figure 2. Subsequently, we obtain charging energies of the individual dots of $E_C^A = e^2/2C_\Sigma$ = 220 μeV and E_C^B = 205 μeV. Thus the 'electronic' radii are r_A = 400 nm and r_B = 430 nm. For the absolute number of electrons in each dot we find that n_A = 850 and n_B = 980. Hence, the dots are rather classical systems in which we do not expect the resolution of discrete single particle energies because of the confinement potential. In the current measurements, the interdot coupling is chosen to be weak (C_{A-B} = 2 aF), i.e. we see a hexagonal array of points for the charging diagram [22] which corresponds to the 'ionic' coupling limit. All results were obtained in the linear regime (drain/source bias V_{ds} = 19 μV).

In an earlier set-up, we focussed on defining a weak link with a modified atomic force microscope (AFM) tip directly in the Al contacts by nano-ploughing the Al sheet and hence forming the Schottky gates [23, 24]. This is of great advantage for probing the microwave response of quantum dots in the absolute near-field limit, since the photon source is located only 100 nm from the tunnel barriers. However, these weak links radiate with a very large radiation linewidth. Hence, we choose here to employ a well characterized JTJ oscillator placed on top of the quantum dots. The JTJ we use in these measurements is an overlap Nb/Al–AlO_x/Nb long Josephson junction with dimensions 20 $\times$ 400 μm^2 (width $\times$ length). In the measurements

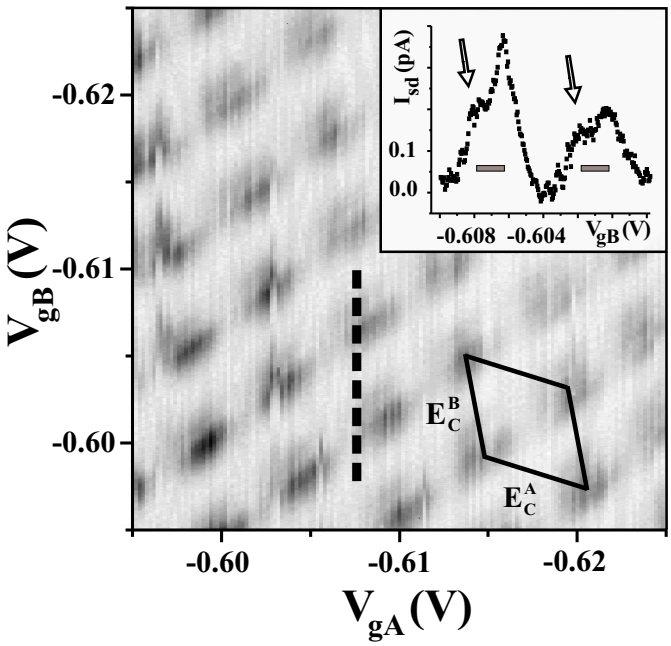

Figure 4. Charging diagram under microwave radiation with the on-chip Josephson oscillator as a source ($f \cong 10$ GHz). The inset shows the photon-induced current through the dot system with the photon-assisted tunnelling resonances. The peak heights and positions are identical to the plots obtained with the far-field source (compare with figure 3). This similar pattern indicates that the coupling of radiation from near- and far-field only depends on the local electrostatic environment.

presented, tuning of the frequency was possible by varying the JTJ critical current with the applied magnetic field and selecting the appropriate bias point at a resonant state. When operated in the flux-flow regime, the JTJ radiation frequencies $f = 2\ \mathrm{eV}/h$ are on the order of 100–500 GHz. This is above the Coulomb energy for this particular quantum dot. We employ a finite magnetic field to operate the junction at a Fiske step of the current–voltage characteristic, a self-resonant state. The fundamental cavity resonance frequency of the junction is $f = \bar{c}/(2\ell)$, where $\bar{c}$ is the Swihart velocity and ℓ is the junction length.

In order to characterize the microwave response of the coupled quantum dots, we first studied them with a conventional microwave source. The radiation was then transduced by an antenna on the gate structure of the quantum dots. The charging diagram of the double dot with microwave excitation is shown as a greyscale plot in figure 3. The radiation of the far-field source is fixed at 10 GHz. The sidebands are found on only one side, depending on the tuning of the barrier transmission coefficients. In measurements on a similar two-dot device, we obtained symmetrically as well as asymmetrically induced sidebands in the charging diagram [25]. However, since we are interested in the alteration of the microwave coupling by the JTJ, we deliberately chose to maintain the tuning with only one sideband, which is clearly visible in the inset of figure 3. This ensures finally that we can directly compare the measurements with the conventional microwave source and the on-chip source. The inset shows one of the typical traces from the greyscale plot with the sidebands induced by the frequency-dependent absorption.

The induced sidebands are marked by arrows—the peak height modulation is due to the specific trace taken out of the charging diagram (marked by the dashed line). A cut along one of the two periodic resonance lines would yield peaks of similar amplitude. The net pumping of electrons leads to a reduction of the absolute current value down to only some 100 fA. Also the noise floor is slightly enhanced by coupling the radiation.

When the on-chip Josephson oscillator is operated as a source with a typical emission frequency of $f \cong 10$ GHz, we observe charging diagrams like the one shown in figure 4. The JTJ emission frequency was determined by taking the I–V characteristics. Biasing the JTJ with a current of $I = 1\ \mu$A, we are able to detect sidebands which resemble those induced by the far-field source (compare the insets of figures 3 and 4). The power emitted is then on the order of $P_{\mathrm{dc}} \sim 20\ \mu\mathrm{V} \times 1\ \mu\mathrm{A} \approx 20$ pW, where 20 μV is the voltage drop over the JTJ at 10 GHz. Moreover, the peak broadening is almost identical to that determined before. As can be seen, the resonances of the current (marked by lines in the plot) and the induced sidebands (marked by arrows) possess a long term stability. Since the observed resonances for the on-chip source as well as for the far-field source are almost identical, we conclude that the photon absorption process only depends on the shape of the local electrostatic potential. Varying the frequency of the radiation for such a tunnel-coupled dot system results in the well-known linear relation between the position of the sideband relative to the ground state and the frequency for the case of weak coupling [11, 25].

In summary, we find photon-assisted tunnelling in a weakly coupled double quantum dot, induced by an on-chip source. This source consists of a long Josephson junction placed on top of the chip carrying the double dot. We find nearly identical radiation coupling with the on-chip source and the far-field source. We conclude from this comparison that the photon absorption process depends only on the local electrostatic environment of the quantum dots. Furthermore, this result confirms that Kohn's theorem is valid in the near-field regime, as long as it provides a spatially homogeneous radiation field across the excited electronic system. This we expect to change when a Josephson junction is embedded in the dot's gate structure.

Acknowledgments

We would like to thank T Klapwijk, S J Allen and D Grundler for extended discussions. This work was funded in part by the Deutsche Forschungsgemeinschaft (DFG), the Defense Advanced Research Projects Agency (DARPA). H Qin would like to thank the Volkswagen-Stiftung for support.

References

[1] Kouwenhoven L P, Jauhar S, Orenstein J, McEuen P L, Nagamune Y, Motohisa J and Sakaki H 1994 *Phys. Rev. Lett.* **73** 3443
[2] Blick R H, Haug R J, van der Weide D W, von Klitzing K and Eberl K 1995 *Appl. Phys. Lett.* **67** 3924
[3] Oosterkamp T H, Kouwenhoven L P, Koolen A E A, van der Vaart N C and Harmans C J P M 1997 *Phys. Rev. Lett.* **78** 1536
[4] Tien P K and Gordon J P 1963 *Phys. Rev.* **129** 647
[5] Stafford C A and Wingreen N S 1996 *Phys. Rev. Lett.* **76** 1916
[6] Ivanov T 1997 *Phys. Rev.* B **56** 12339
Stoof T H and Nazarov Yu V 1996 *Phys. Rev.* B **53** 1050

[7] Grifoni M and Hänggi P 1998 *Phys. Rep.* **304** 229
[8] Inarrea J, Platero G and Tejedor C 1994 *Phys. Rev.* B **50** 4581
[9] Nakamura Y, Pashkin Yu A and Tsai J S 1999 *Nature* **398** 786
[10] Blick R H, van der Weide D W, Haug R J and Eberl K 1998 *Phys. Rev. Lett.* **81** 689
[11] Oosterkamp T H, Fujisawa T, van der Wiel W G, Ishibashi K, Hijman R V, Tarucha S and Kouwenhoven L P 1998 *Nature* **395** 873
[12] Adourian A S, Yang S and Westervelt R M, Chapman K L and Gossard A C 1998 *J. Appl. Phys.* **84** 5808
[13] Visscher E H, Schraven D M, Hadley P and Mooij J E cond-mat/9904382
[14] Ustinov A V 1998 *Physica* D **123** 315–29
[15] Koshelets V P, Shitov S V, Shukin A V, Filippenko L V, Mygind J and Ustinov A V 1997 *Phys. Rev.* B **56** 5572
[16] Koshelets V P, Shitov S V, Filippenko L V, Baryshev A M, Golstein H, de Graauw T, Luinge W, Schaeffer H and van de Stadt H 1996 *Appl. Phys. Lett.* **68** 1273
[17] Kohn W 1961 *Phys. Rev.* **123** 1242
[18] Pfannkuche D and Ulloa S E 1995 *Phys. Rev. Lett.* **74** 1194
Weis J, Haug R J, von Klitzing K and Ploog K 1993 *Phys. Rev. Lett.* **71** 4019
[19] Sikorski C H and Merkt U 1989 *Phys. Rev. Lett.* **62**, 2164
Demel T, Heitmann D, Grambow P and Ploog K 1990 *Phys. Rev. Lett.* **64** 788
Merkt U 1996 *Phys. Rev. Lett.* **76** 1134
Bakshi P, Broido D A and Kempa K 1990 *Phys. Rev.* B **42** 7416
[20] Fujisawa T and Tarucha S 1997 *Superlatt. Microstruct.* **21** 247-254
[21] Novotny L 1996 *Appl. Phys. Lett.* **69** 3806
[22] Livermore C, Crouch C H, Westervelt R M, Campman K L and Gossard A C 1996 *Science* **274** 1332
[23] Irmer B, Blick R H, Simmel F, Gödel W, Lorenz H, and Kotthaus J P 1998 *Appl. Phys. Lett.* **73** 2061
[24] Irmer B, Simmel F, Blick R H, Lorenz H, Kotthaus J P, Bichler M and Wegscheider W 1999 *Superlatt. Microstruct.* **25** 785
[25] Qin H, Blick R H, Simmel F, Holleitner A W, Kotthaus J P and Eberl K 2000 *Phys. Rev.* submitted